Critical coupling of surface plasmons in graphene attenuated total reflection geometry

Mauro Cuevas[a,b,*],

[a] *Consejo Nacional de Investigaciones Científicas y Técnicas (CONICET) and Facultad de Ingeniería y Tecnología Informática, Universidad de Belgrano, Villanueva 1324, C1426BMJ, Buenos Aires, Argentina*

[b] *Grupo de Electromagnetismo Aplicado, Departamento de Física, FCEN, Universidad de Buenos Aires and IFIBA, Ciudad Universitaria, Pabellón I, C1428EHA, Buenos Aires, Argentina*

Abstract

We study the optical response of an attenuated total reflection (ATR) structure in Otto configuration with graphene sheet, paying especial attention to the occurrence of total absorption. Our results show that due to excitation of surface plasmons on the graphene sheet, two different conditions of total absorption may occur. At these conditions, the energy loss of the surface plasmon by radiation is equal to its energy loss by absorption into the graphene sheet. We give necessary conditions on ATR parameters for the existence of total absorption.

Keywords: surface plasmon, graphene, attenuated total reflection
PACS: 81.05.ue, 73.20.Mf, 78.68.+m, 42.25.Ja

The localization provided by surface plasmons (SPs) is very attractive for many applications such as data storage, microscopy, light generation or biophotonics [1, 2]. Apart from the well known SPs supported by an insulator–metal interface, long living SPs can be supported by graphene –a 2 D sheet of carbon atoms organized in a honeycomb lattice– from terahertz up to mid–infrared frequencies [3]. High confinement, relative low loss, and the ability of tuning the SP spectrum through electrical or chemical modification of the carrier density, makes the graphene a promising plasmonic alternative material to noble metals at long wavelengths [4, 5]. Phase–coupling techniques which give the photon the additional propagation constant increase needed to achieve SP excitation have been extensively used. One of the most popular coupling techniques is based on the use of attenuated total reflection (ATR) which requires the introduction of a second surface, usually the base of a prism, as shown in Figure 1 for the Otto configuration [6, 7]. The excitation of SPs causes a pronounced minimum in the reflectivity which may reach zero value (total absorption condition) for optimized ATR structures [6, 8].

In this letter, we report the main results of our theoretical study about the total absorption phenomenon in an ATR system in Otto configuration with graphene monolayer. By applying energy conservation in a finite–size region, we demonstrate that critical coupling in which the incident radiation is totally absorbed is achieved when the energy loss of the SP by radiation into the prism is equal to its energy loss by absorption into the graphene monolayer. This result is in accord with those obtained in Ref. [9] by applying a different method and for a metallic ATR structure. In addition, it is found that the reflection coefficient can have two zeros for two different angles of incidence and thicknesses of the vacuum layer (or chemical potentials on the graphene monolayer). In [10], it was reported that the reflectivity of an ATR system in Otto configuration may have two zeros, but only one of them is caused by excitation of SPs. In contrast, we show that the two zeros found here are due to the excitation of SPs on the graphene monolayer. Furthermore, we give necessary conditions on ATR parameters for the existence of total absorption. The Gaussian system of units is used and an $\exp(-i\,\omega\,t)$ time–dependence is implicit throughout the paper, with ω as the angular frequency, t as the time, and $i = \sqrt{-1}$.

Figure 1 shows the Otto–ATR structure. Medium 2 is vacuum in contact with two nonmagnetic dielectric materials ($\mu_1 = \mu_3 = 1$) with real and positive electric permittivities (ε_1, ε_3). A SP can be excited along the graphene monolayer located at interface 2–3 when the incident plane wave reaches the base of the prism (interface 1–2) with an angle θ greater than the critical angle of total reflection. To illustrate this coupling mechanism, we study the electromagnetic response of the ATR structure when excited by an plane wave (plane wave scattering problem, or reflectivity problem). On the other hand, this coupling is reciprocal, *i.e.*, the SP propagating by the graphene monolayer in $+x$ direction radiates away from the vacuum layer in the form of a beam that progresses at an angle θ in the prism region, as shows figure 1. This fact leads to radiation losses which are expressed as an increase of the imaginary part of the SP propagation constant. To obtain all the propagation characteristics of SPs in the ATR system, we study the non–trivial solutions to the boundary value problem in the absence of incident fields (guided–wave eigenvalue problem, or eigenmode problem).

For p polarization the magnetic field of the electromagnetic eigenmodes is parallel to the z axis, $\mathbf{H} = e^{i\alpha x}\, h(y)\, \mathbf{z}$, where α is

*corresponding author
Email address: cuevas@df.uba.ar (Mauro Cuevas)

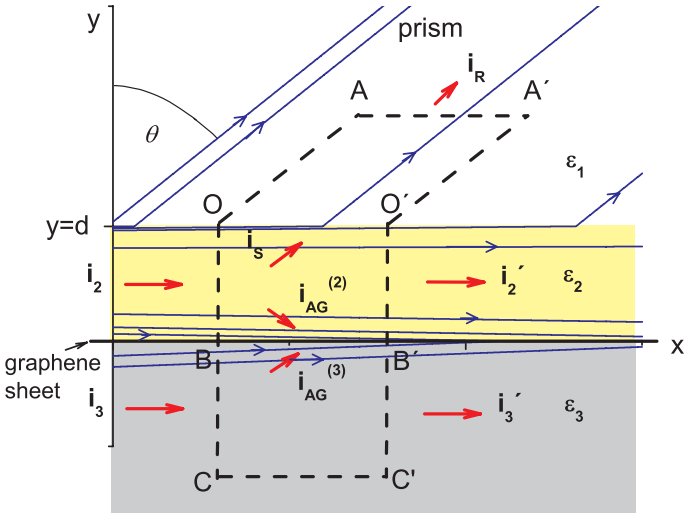

Figure 1: (Color online) Schematic illustration of the ATR geometry. The graphene sheet is located at $y = 0$ interface, between media 2 and 3. Closed region where energy conservation is applied (dashed line). Lines of Poynting vector flux are plotted (blue lines) for $\omega/c = 0.025\mu\text{m}^{-1}$ and thickness $d = 0.026\lambda$. $\varepsilon_1 = 16$, $\varepsilon_2 = 1$, $\varepsilon_3 = 3.9$ and graphene parameters are $\mu_c = 0.35\text{eV}$, $\gamma = 0.1\text{meV}$ and $T = 300\text{K}$.

the propagation constant of the ATR eigenmodes and

$$h(y) = \begin{cases} r_1\, e^{i\beta^{(1)}y} & y > d, \\ \left[r_2\, e^{i\beta^{(2)}y} + t_1\, e^{-i\beta^{(2)}y}\right] & 0 < y < d, \\ t_2\, e^{-i\beta^{(3)}y} & y < 0. \end{cases} \tag{1}$$

Here, r_j and t_j $(j = 1, 2)$ are complex magnitudes, and $\beta^{(j)} = \sqrt{k_0^2\varepsilon_j - \alpha^2}$ $(j = 1, 2, 3)$ is the component in the y direction of the wave vector in each of the media, $k_0 = \omega/c$ is the modulus of the photon wave vector in vacuum, ω is the angular frequency and c is the vacuum speed of light. The electric field $\mathbf{E} = e^{i\alpha x}\,\mathbf{e}(y)$ are easily written also as functions of r_j and t_j by means of a Maxwell curl equation, where

$$\mathbf{e}(y) = \begin{cases} \frac{r_1}{k_0\varepsilon_1}[-\beta^{(1)}\mathbf{x} + \alpha\mathbf{y}]e^{i\beta^{(1)}y} & y > 0, \\ \frac{1}{k_0\varepsilon_2}[-\beta^{(2)}(t_1 e^{i\beta^{(2)}y} - r_2 e^{-i\beta^{(2)}y})\mathbf{x} & \\ \quad +\alpha(t_1 e^{i\beta^{(2)}y} + r_2 e^{-i\beta^{(2)}y})\mathbf{y}] & 0 < y < d, \\ \frac{t_2}{k_0\varepsilon_3}[\beta^{(3)}\mathbf{x} + \alpha\mathbf{y}]e^{-i\beta^{(3)}y} & y < 0. \end{cases} \tag{2}$$

There are two types of boundary conditions which must fulfill the solutions given by Eqs. (1) and (2), boundary conditions at $y = \pm\infty$ and boundary conditions at interfaces $y = 0$ and $y = d$. The former requires either outgoing waves at infinity or exponentially decaying waves at infinity, depending on the values of α and $k_0\sqrt{\varepsilon_j}$ [12]. The boundary conditions at $y = d$ require the continuity of the tangential components of the electric field and the magnetic field. The boundary conditions at $y = 0$ require the tangential component of the electric field to be continuous and the tangential component of the magnetic field to be discontinuous across the interface by an amount whose magnitude is equal to the magnitude of the surface current density on graphene sheet [5, 11]. Applying these conditions in Eqs. (1) and (2) we obtain a homogeneous system for the four unknown coefficients r_j and t_j $(j = 1, 2)$ [5]. The dispersion equation for the propagation constant α can be obtained by requiring the determinant D of this system to be zero, a condition that can be written as

$$\begin{aligned} D = &(Z_1 + Z_2)\,(Z_2 + Z_3 W_2^+) \\ &+ (Z_1 - Z_2)\,(Z_2 - Z_3 W_2^-)\, e^{i2\beta^{(2)}d} = 0, \end{aligned} \tag{3}$$

where $Z_j = \frac{\beta^{(j)}}{\varepsilon_j}$, $W_2^{\pm} = 1 \pm \frac{4\pi\sigma}{ck_0} Z_2$ and σ is the conductivity of the graphene sheet given by the Kubo formula [11]. It should be noted that the eigenvalue α is complex–valued, where $\text{Im}\alpha$ is the spatial decay rates and it represents the total damping of the eigenmode. In addition to SPs, there also exist eigenmodes having $|\text{Re}\,\alpha| < k_0$. In this case, the field inside the vacuum layer propagates along x direction bouncing between the two boundaries at $y = 0$ and at $y = d$ before it loses most of its energy by refraction, *i.e.*, by radiation into the semi infinite regions above $(y > d)$ and below $(y < 0)$ the vacuum layer. In this paper we confine our attention to just SPs which are evanescent waves in the vacuum layer and in the semi infinite region $y < 0$.

Since Eq. (3) gives two complex solutions differing in sign (for propagation along $\pm x$), we have chosen the one with $\text{Re}\,\alpha > 0$. For conventional media, in this case dielectric media 1, 2 and 3, the physically correct Riemann sheet gives $\text{Im}\,\alpha \geq 0$ [12].

After calculating α, we obtain the field amplitudes r_2, t_1, and t_2 in Eq. (1) as a function of r_1. As both the magnetic and the electric SP fields depend on x axis in the form $e^{i\alpha x}$, the time–averaged Poynting vector thus reads

$$\langle \mathbf{S} \rangle = \frac{c}{8\pi}\,\text{Re}\,(\mathbf{E} \times \mathbf{H}^*) = e^{-2\text{Im}\alpha x}\mathbf{s}(y), \tag{4}$$

where the asterisk denotes the complex conjugate and $\mathbf{s}(y) = \mathbf{e}(y) \times \mathbf{z}h^*(y)$. In the second equality in Eq. (4) we have taken into account that α is a complex number. According with Eq. (4), surface plasmons are attenuated as propagate along $+x$ direction. The attenuation is due by two damping processes, namely, energy radiation and energy absorption. This means that, as the SP propagates along the graphene sheet, part of the energy it carries can be radiated into the prism and the other part is absorbed in the graphene sheet. In the proximity of the graphene surface, the lines of Poynting vector flux are almost parallel to the x–axis. Due to absorption losses in the graphene sheet, a small number of lines finish on this surface, as can be seen in figure 1, where we have plotted the lines of Poynting vector for $\omega/c = 0.025\mu\text{m}^{-1}$ and for a thickness $d = 0.026\lambda$ ($\lambda = 2\pi\, c/\omega$ is the photon wavelength). The presence of surface 1–2 at the base of the prism is manifested in the existence of current lines that emerge from the surface in region $y > d$ in the form of radiation flow. The density of these lines along the propagation direction decreases as a consequence of the decrease in the power density carried by the SP. These lines can be verified to form an angle θ with the y–axis given by the relation $\omega/c\,\sqrt{\varepsilon_1}\sin\theta = \text{Re}\,\alpha$.

In considering the energy balance in the region $OAA'O'B'C'CB$ of Figure 1, lines OA and $O'A'$ are taken to be parallel to the radiation direction. As a consequence, the energy flows i_1 through the line OA and i_1' through the line $O'A'$ are equal to zero. The total incident energy flow reaching

the region $CBOA$ has two parts: the flow i_3 through the line CB in the lower medium 3 and the incident energy flow i_2 through the line BO in the medium 2. One part $i_{ag}^{(2)}$ of the incident energy flow i_2 is absorbed by the graphene sheet and another part i_s is transmitted to the medium 1 through the line OO'. A third part $i_2^{'}$ is transmitted through the line $O'B'$. Taking into account Eq. (4), we can see that this part is $i_2^{'} = i_2\, e^{-2\,\mathrm{Im}\,\alpha\, X}$, where X is the length of the segment AA' . Since the medium 2 is lossless, the energy conservation in region $BOO'B'$ is written as

$$i_2(1 - e^{-2\,\mathrm{Im}\,\alpha\, X}) = i_s + i_{ag}^{(2)}. \tag{5}$$

Taking into account that $i_1 = i_1^{'} = 0$, the energy conservation in region $OAA'O'$ gives $i_s = i_r$ and Eq. (5) is rewritten as

$$i_2(1 - e^{-2\,\mathrm{Im}\,\alpha\, X}) = i_r + i_{ag}^{(2)}, \tag{6}$$

where i_r is the energy flow radiated by the SP. On the other hand, one part $i_{ag}^{(3)}$ of the energy flow i_3 is absorbed by the graphene sheet, a second part $i_3^{'} = i_3\, e^{-2\,\mathrm{Im}\,\alpha\, X}$ is transmitted through the line $C'B'$ and a third part i_t is transmitted through the line CC'. Due to evanescent character of the field in medium 3, as CB tends to infinite, then i_t tends to zero. Therefore, the energy conservation in region $CBB'C'$ is written as

$$i_3(1 - e^{-2\,\mathrm{Im}\,\alpha\, X}) = i_{ag}^{(3)}. \tag{7}$$

If we divide Eqs. (6) and (7) by the energy $i_a = (i_2 + i_3)(1 - e^{-2\,\mathrm{Im}\,\alpha\, X})$ leakage into the region $OAA'O'B'C'CB$, we obtain

$$\frac{i_2}{i_2 + i_3} = \frac{i_r}{i_a} + \frac{i_{ag}^{(2)}}{i_a}, \tag{8}$$

and

$$\frac{i_3}{i_2 + i_3} = \frac{i_{ag}^{(3)}}{i_a}. \tag{9}$$

By adding Eqs. (8) and (9) we obtain the energy conservation in the region $OAA'O'B'C'CB$

$$1 = \frac{i_r}{i_a} + \frac{i_{ag}}{i_a}, \tag{10}$$

where $i_{ag} = i_{ag}^{(2)} + i_{ag}^{(3)}$ is the total energy flow absorbed by the graphene sheet.

Figures 2a and 2b show the real and the imaginary parts of the nondimensional propagation constant $\kappa = c\,\alpha/\omega$ as a function of d/λ ($\lambda = 250\mu$m) at $\omega/c = 0.025\mu\mathrm{m}^{-1}$ ($\omega = 7.5$THz) and for $\mu_c = 0.35$eV. For values of $d/\lambda \geq 0.11$, both functions $\mathrm{Re}\,\kappa(d/\lambda)$ and $\mathrm{Im}\,\kappa(d/\lambda)$ take a value that is almost constant and equal to the corresponding values at $d/\lambda \to \infty$. This shows that both the phase velocity and the surface plasmon energy losses are essentially those corresponding to a single graphene sheet sandwiched between two dielectric half space with permitivities ε_2 and ε_3, where the surface plasmon does not radiate. As the thickness d is reduced ($d/\lambda < 0.11$), $\mathrm{Re}\,\kappa(d/\lambda)$ increases significantly, indicating a decrease in the surface phase velocity, whereas $\mathrm{Im}\,\kappa(d/\lambda)$ increases until it reaches a maximum value at $d/\lambda \approx 0.0153$, and then decreases. Figure 2c shows the energy absorbed in the graphene sheet and the energy radiated into the upper medium, both normalized with respect to the total energy leakage i_a, as a function of d/λ. These curves intersect at thicknesses $d = 0.01268\,\lambda$ and $d = 0.02609\,\lambda$, indicating that a critical coupling in which the intrinsic damping of the surface plasmon equals its radiative damping occurs at two different conditions (power–matched condition). Under these

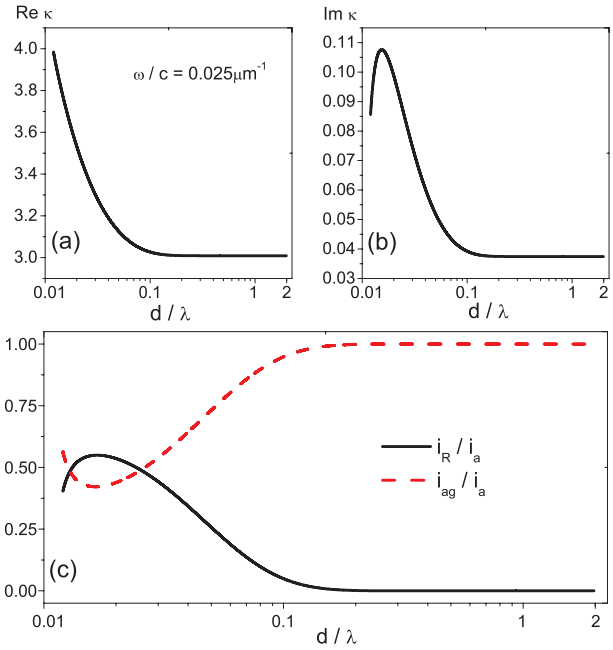

Figure 2: (Color online) (a) Real and (b) imaginary parts of the nondimensional surface plasmon propagation constant κ for different thickness d and for $\omega/c = 0.025\mu\mathrm{m}^{-1}$ ($\omega \approx 7.5$THz). (c) i_{ag}/i_a and i_r/i_a as a function of d/λ. $\varepsilon_1 = 16$, $\varepsilon_2 = 1$, $\varepsilon_3 = 3.9$ and graphene parameters are $\mu_c = 0.35$eV, $\gamma = 0.1$meV and $T = 300$K.

conditions we expect that when a p–polarized plane wave is impinging from region $y > d$, all the incoming radiation be absorbed at resonance. This fact can be confirmed by studying the reflectivity problem in which an incident plane wave is coming under the angle θ to the y axis. The complex amplitude r_1 of the fields reflected in medium 1 can be obtained by following steps formally similar to those already presented to calculate the magnitude denoted by the same name in the eigenmode problem, adding to the fields in region $y > d$ in Eqs. (1) and (2) a term which takes into account the presence of the incident plane wave. The boundary conditions are the same as in the eigenvalue problem but the scattered field must satisfy the radiation condition at $y = \pm\infty$. Under these hypotheses, the complex amplitude r_1 of the fields reflected in medium 1 results $r_1 = N/D$, where

$$N = (Z_1 - Z_2)\,(Z_2 + Z_3 W_2^{+}) + (Z_1 + Z_2)\,(Z_2 - Z_3 W_2^{-})\, e^{i2\beta^{(2)} d}. \tag{11}$$

It is noteworthy that whereas in the eigenmode problem previously analized α is a complex magnitude that represents the propagation constant of an SP, in the reflectivity problem α takes a real value imposed by the incident plane wave, α =

$k_0\sqrt{\varepsilon_1}\sin\theta$. When the condition $k_0\sqrt{\varepsilon_1}\sin\theta = \mathrm{Re}\alpha$ holds, we expect an energy transfer from the incident wave to the SP and therefore a decrease in the reflectivity of the system. Figure 3a shows the reflectivity $|r_1|^2$ as a function of the angle of incidence θ for two thicknesses $d/\lambda = 0.01268$ and $d/\lambda = 0.02609$, which correspond to the power–matching condition. Although curves with a pronounced dip (computed minima 10^{-6}) can be observed at an angle of incidence $\theta \approx 57.35°$ for $d/\lambda = 0.02609$, and $\theta \approx 77°$ for $d/\lambda = 0.01268$, we confirm the total absorption condition by a more rigorous way based on the computation in the complex plane of the zeros of the reflection coefficient (zeros of Eq. (11)), *i.e.*, by calculating the complex zero $z_0 = \sin\theta_0$, where θ_0 is the extension to the complex plane of the angle of incidence where the reflection coefficient is zero, as a parametric function of d/λ and for the same parameters as in Figure 2. As the value of d/λ is changed, the positions of the zero determine a trajectory in the complex plane. This trajectory cross the real axis (where θ_0 is real) for some critical value of d/λ where the total absorption phenomenon occur. Figure 3b shows the parametric trajectory of $z_0(d/\lambda)$ for

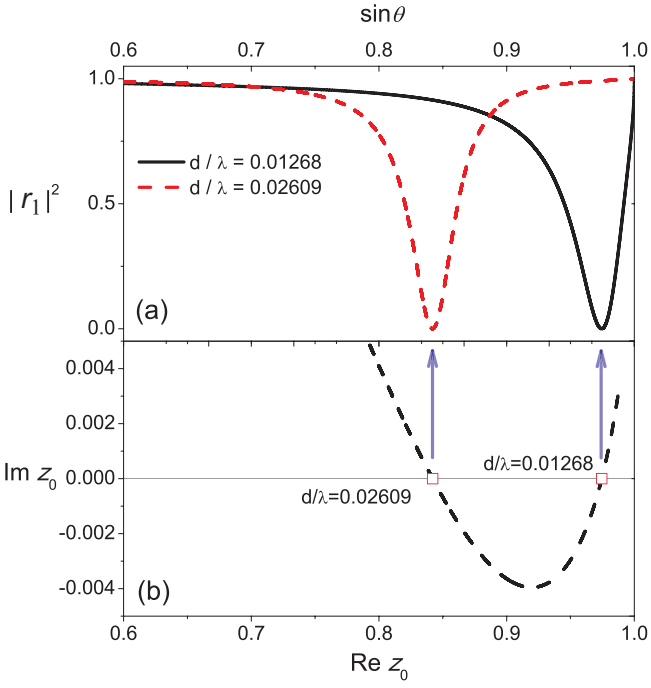

Figure 3: (Color online) (a) Reflectivity $|r_1(\sin(\theta))|^2$ as a function of the sine of the angle of incidence θ and for the two values of the thickness d/λ where the two damping processes, surface plasmon radiation and surface plasmon absorption, are of equal magnitude (power matched condition $i_r = i_{ag}$). (b) Trajectory of the zero of the reflectivity in the complex plane as a function of d/λ ($z_0(d/\lambda)$). Frequency and constitutive parameters are the same as in Figure 2

$0.012 < d/\lambda < 0.043$. When d/λ is increasing, the imaginary part of z_0 changes its sign at a critical value of d/λ between $d/\lambda = 0.01267$ and $d/\lambda = 0.01269$, for which the reflectivity is null. The trajectory of Figure 3b shows that the imaginary part of z_0 changes its sign again, at a critical value of d/λ between $d/\lambda = 0.02608$ and $d/\lambda = 0.02610$, indicating a new condition of total absorption.

It is well known that it is possible to tune the ATR conditions by changing the chemical potential μ_c of the graphene monolayer [6]. Following a similar procedure as used to determine the complex zeros as a parametric function of thickness d, by varying the value of μ_c (mantaining fixed the value of d), one can obtain the trajectory of the zero in the complex plane as a parametric function of μ_c. When this trajectory crosses the real axis, the total absorption phenomenon occur for a critical value of μ_c. Thereby, the total absorption condition, *i.e.* the power matched condition, can be tuned by changing geometric or electrical parameters (the thickness of the vacuum layer or the chemical potential). We set $r_1 = 0$ and obtain how the values of μ_c change with the values of d/λ . In Figure 4a we plot the pair of these two variables giving $r_1 = 0$ for $\omega/c = 0.01,\ 0.025$ and $0.04\mu\mathrm{m}^{-1}$.

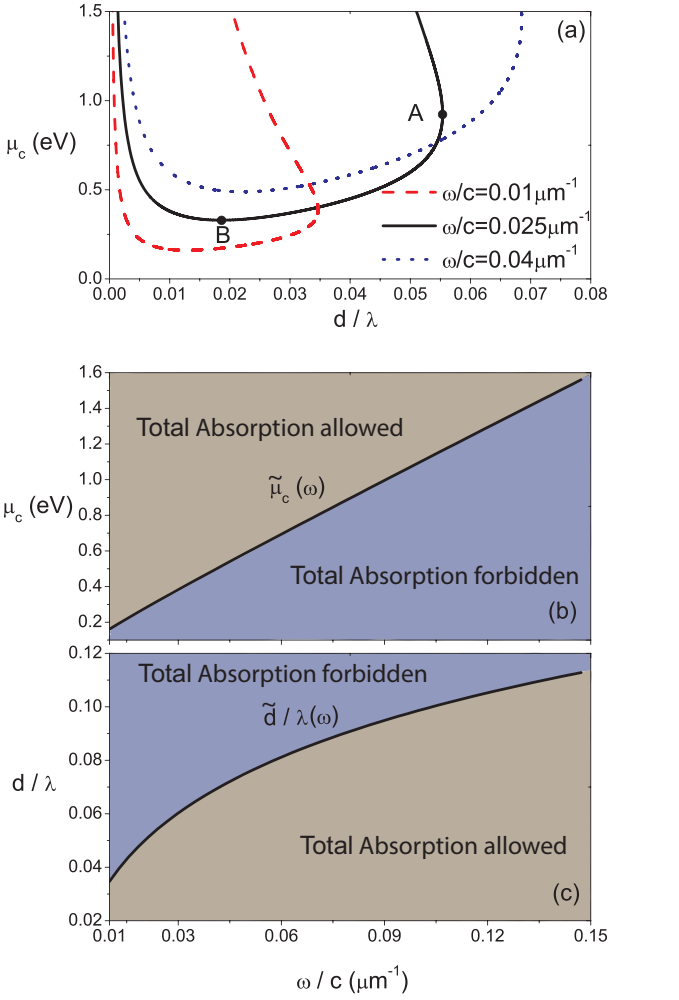

Figure 4: (Color online) (a) Thickness d/λ, and chemical potential μ_c, corresponding to zero reflectivity of the ATR structure for frequencies $\omega/c = 0.01,\ 0.025$ and $0.04\mu\mathrm{m}^{-1}$. Regions of the plane (b) $\mu - \omega/c$ and (c) $d/\lambda - \omega/c$ for which total absorption occur. (b) and (c) show a plot of $\widetilde{\mu_c}$ and $\widetilde{d}/\lambda$, both as a function of frequency, respectively.

From this figure, it can be seen that there are a maximum value of d/λ ($\widetilde{d}/\lambda$) and a minimum value of μ_c ($\widetilde{\mu_c}$), both quantities depending of frequency, for which the total absorption phenomenon occur. For instance, for $\omega/c = 0.025\mu\mathrm{m}^{-1}$ the maximum thickness value is $\widetilde{d} = 0.05537\lambda$ and the correspond-

ing chemical potential $\mu_c = 0.92431$eV (point A in figure 4a). As we move along the curve from the point A, by decreasing the value of μ_c, we arrive to the point B where the minimum value of the chemical potential $\widetilde{\mu_c} = 0.32949$eV for the occurrence of total absorption is reached. It is worth noting that for values of μ_c lower than $\widetilde{\mu_c}$ or for values of d larger than $\widetilde{d}$, the total absorption phenomenon is forbidden. Figure 4b shows the curve of $\widetilde{\mu_c}$ as a function of frequency, which separates the region where total absorption occur for two conditions from region where such phenomenon is forbidden. When μ_c lies on the boundary curve $\widetilde{\mu_c}(\omega/c)$, the two zeros of the reflection coefficient coincide. Similarly, we found that, when thickness d/λ lies bellow or above the curve of $\widetilde{d}/\lambda$ as a function of frequency in Figure 4c, the reflectivity can have zeros (one or two zeros) and no zero, respectively.

In conclusion, we have investigated the occurrence of total absorption in an Otto–ATR system with graphene monolayer. By calculating the complex zeros of the reflectivity and by solving the dispersion relation for the complex propagation constant of SPs, we have demonstrated that this phenomenon can be achieved for two different resonant conditions. When the chemical potential of the graphene monolayer is maintained fixed, these conditions can appear at two angles of incidence and thicknesses of the vacuum layer, while if the thickness of the vacuum layer is fixed, these conditions can appear at two angles of incidence and chemical potentials. We have demonstrated that in these resonant conditions the total absorption phenomenon occurs when the power radiated by the SP is equal to the power absorbed into the graphene monolayer. Furthermore, we have calculated the value of $\widetilde{\mu_c}(\omega/c)$ and of $\widetilde{d}/\lambda(\omega/c)$ which separates the region where total absorption occur from region where such phenomenon is forbidden.

The author acknowledge the financial support of Consejo Nacional de Investigaciones Científicas y Técnicas, (CONICET, PIP 451).

[1] S. A. Maier *Plasmonics: Fundamentals and Applications* (New York: Springer, 2007).
[2] W. L. Barnes, A. Dereux, T. W. Ebbesen, Nature 424, 824 (2003).
[3] A. Geim, K. Novoselov, Nat. Mater 6, 183 (2007).
[4] J. Jablan, M. Soljacic, H. Buljan, Proc. IEEE 101, 1689 (2013).
[5] Y. V. Bludov, A. Ferreira, N. M. R. Peres, and M. I. Vasilevskiy, Int. J. Mod Phys B 27 (2013)
[6] Y. V. Bludov, M. I. Vasilevskiy and N. M. R. Peres, EPL, 92 68001 (2010)
[7] C. H. Gan, Applied Physics Letters 101, 111609 (2012).
[8] L. Wang, Li–Gang Wang, Lin–Hua Ye, M. Al–Amri, Shi–Yao Zhu, and M. S. Zubairy, Phys. Rev. A 94, 013806 (2016).
[9] H. Raether, *Surface Plasmons on Smooth Rough Surface and on Gratings* (Springer-Verlag, 1988).
[10] W. Lukosz and H. Wahlen, Optics Letters 3 (1978).
[11] M. Cuevas, Journal of Optics 18, 105003 (2016).
[12] M. Zeller, M. Cuevas, and R. A. Depine, J. Opt. Soc. Am. B 28 (2011).